processes

MDPI

Article

Measuring Variable Discharge Under Partially Full Pipe Flow

Vasiliki Koutsospyrou [1], Graham Sander [1,*], Ashraf El-Hamalawi [1], Duncan Wallace [2] and Martin Croft [2]

[1] School of Architecture, Building and Civil Engineering, Loughborough University, Loughborough LE11 3TU, UK; v.koutsospyrou2@lboro.ac.uk (V.K.); a.el-hamalawi@lboro.ac.uk (A.E.-H.)
[2] Dynamic Flow Technologies Ltd., Loughborough DE1 1TJ, UK; duncan@des19n.com (D.W.); martin@des19n.com (M.C.)
* Correspondence: g.sander@lboro.ac.uk

Abstract: Accurately measuring the discharge in partially full pipe flow is both difficult and demanding. In this regard, a new meter sensor using microwave technology has been evaluated for determining partially full pipe discharge across a range of flow depths. A range of experiments with smooth PVC pipes of two different pipe diameters (101.6 and 152.4 mm) at two different pipe slopes (1° and 2°) were carried out under turbulent (Reynolds numbers = (0.27–3.25) $\times$ 10^5) and supercritical flows with Froude numbers F_r in the range of $1.5 \leq F_r \leq 3.6$. Our results showed that when combining the microwave sensor readings with either the Chezy equation or Manning's law, reliable discharge predictions were found compared to the measured discharge across all experiments. The range of R^2 values obtained from the plots of predicted versus measured discharge were all greater than 97%, indicating an accuracy allowing the meter to be used in commercial applications.

Keywords: partial full pipe-flow; microwave; sensor; Chezy; Manning; ColeBrook-White; discharge

check for updates

Academic Editors: Valentina E. Balas and Rajeeb Dey

Received: 12 February 2025
Revised: 25 March 2025
Accepted: 2 April 2025
Published: 4 April 2025

Citation: Koutsospyrou, V.; Sander, G.; El-Hamalawi, A.; Wallace, D.; Croft, M. Measuring Variable Discharge Under Partially Full Pipe Flow. *Processes* **2025**, *13*, 1089. https://doi.org/10.3390/pr13041089

Copyright: © 2025 by the authors. Licensee MDPI, Basel, Switzerland. This article is an open access article distributed under the terms and conditions of the Creative Commons Attribution (CC BY) license (https://creativecommons.org/licenses/by/4.0/).

1. Introduction

Flow in partially filled pipe is analogous to open channel flow in that it is primarily driven by gravity. While it has received far less attention than pressured full pipe flow, nonetheless there are important engineering applications within (i) the transport of wastewater in sewers, (ii) the transport of slurries in mining and nuclear industries, and (iii) road-crossing culverts [1–3]. Determining the flow in partially filled pipes is a challenging measurement environment where the entire range from very low to nearly full pipe flows can occur. This is primarily due to the significant variation in the cross-sectional fluid flow velocity. The level of variation has been shown quite clearly in studies by Refs. [1,2,4,5]. Partially filled pipe flow is usually "treated" as open channel flow, and the area velocity method is the most commonly used approach for flow measurement [6]. They found that to obtain an accurate measurement of flow in the pipes, an understanding of the mean, average, and maximum stream-wise velocity distributions for various flow conditions, i.e., laminar and turbulent, as well as frictional losses and values of Manning's coefficient n, was essential. However, in experiments by Ref. [7] on partially full smooth-walled pipes, they concluded that the use of Manning's n in small-diameter (i.e., 100 mm) partially filled smooth pipes is unsuitable. Instead, they found that the Colebrook–White formula provided improved predictions of maximum depth and velocity along the pipe.

In Ref. [5], particle imaging velocimetry (PIV) was used to investigate the mean stream-wise velocity distribution and friction factor values in a smooth circular open channel. Their data showed that flow characteristics vary whether the flow depth is higher

or lower than 50% of the pipe diameter. They stated that "even though [the] mean and maximum velocities increase with flow depth, the ratio of mean to maximum velocities decreases when the flow depth is lower than 50%, whereas it is nearly identical for higher flow depths [greater than 50%]". According to the authors, the Chézy *C* and Manning's *n* coefficients vary significantly for flow depths below 50%. This is because of the relatively larger frictional force, compared to a smaller mean velocity, which reduces as flow depth increases.

Consequently, accurate flow measurement in partially full pipes is a difficult task, especially when flow meters rely on measuring velocities. With respect to wastewater collection systems, they require measurement capabilities for the real-time control of flows, as well as for performance evaluation in line with European regulations. At present, sewer flow is almost completely confined to short-term and investigative measurements and is undertaken mainly by electromagnetic or Doppler measurements. Electromagnetic flow meters require full pipes, and they are a contact method of measurement, i.e., the flow meter/sensor is in contact with the fluid. A drawback of the Doppler flow meters is that the velocity profile they are measuring is not uniform and depends not only on upstream and downstream arrangements but also on water levels, flow rates, and wall conditions, and therefore need to be corrected to obtain the averaged velocity [8].

Acoustic reflectometry survey techniques are a contact method and cost considerably less than other techniques [9]. While they are also quicker and simpler to use, this technique only yields a limited number of measurements in a cross-section [10]. Choosing a measuring section for flow contact methods may be difficult, as it is necessary to take both hydraulic conditions and practical criteria into account, such as accessibility, safety of staff, equipment, and connection to electrical and communication networks.

In an effort to overcome these problems, a new microwave meter (MWM), shown in Figures 1–4, was developed by Dynamic Flow Technologies Ltd. (Loughborough, UK) and tested at the Fluid Mechanics Laboratories of Loughborough University. Microwave analysis can be applied to suit a wide range of requirements and has a number of advantages over competing technologies, especially for wastewater sensing applications. This includes capabilities to measure non-destructively true real-time sensing and direct sample measurement, i.e., continuous sampling [11], a feature currently unavailable in many competing technologies.

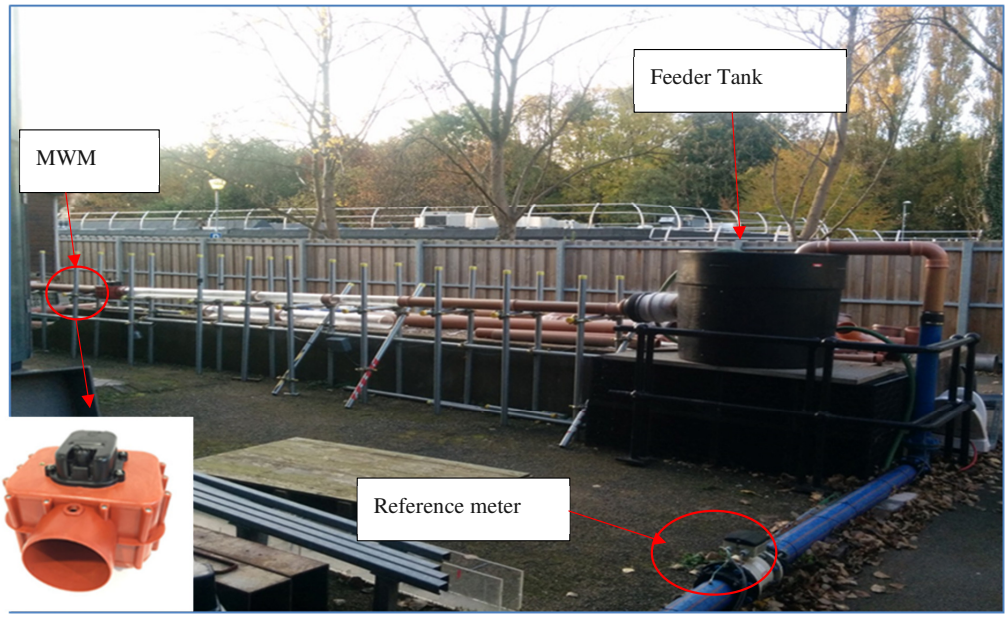


Figure 1. Test rig encompassing mainly the pipe system supported on scaffolding and the feeder tank.

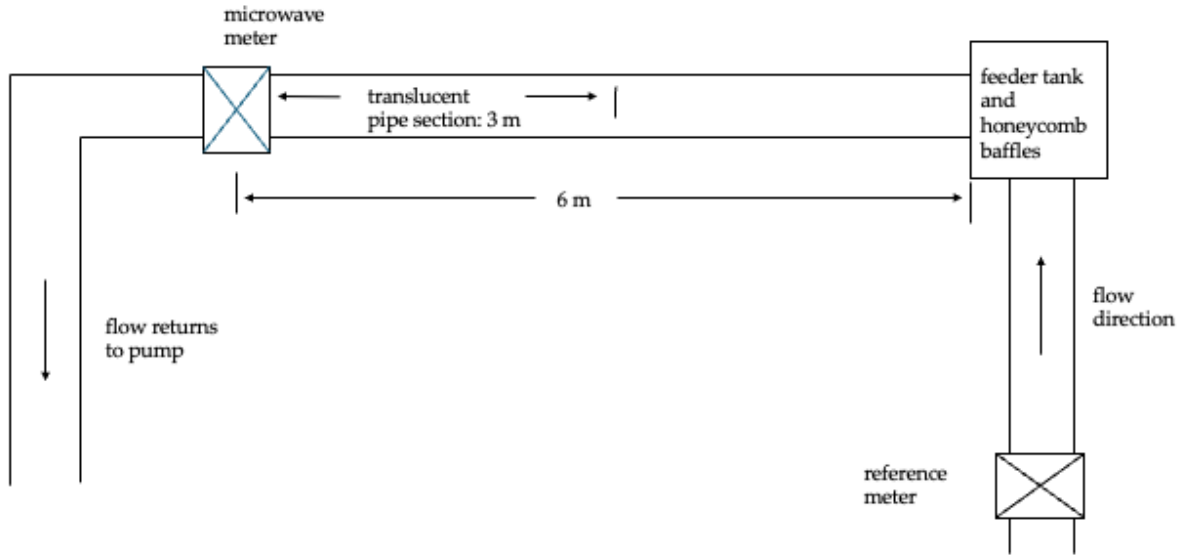


Figure 2. Schematic representation of the experiment showing relative positions of the reference and microwave meters, flow direction, and section of translucent pipe. Distances are not drawn to scale.

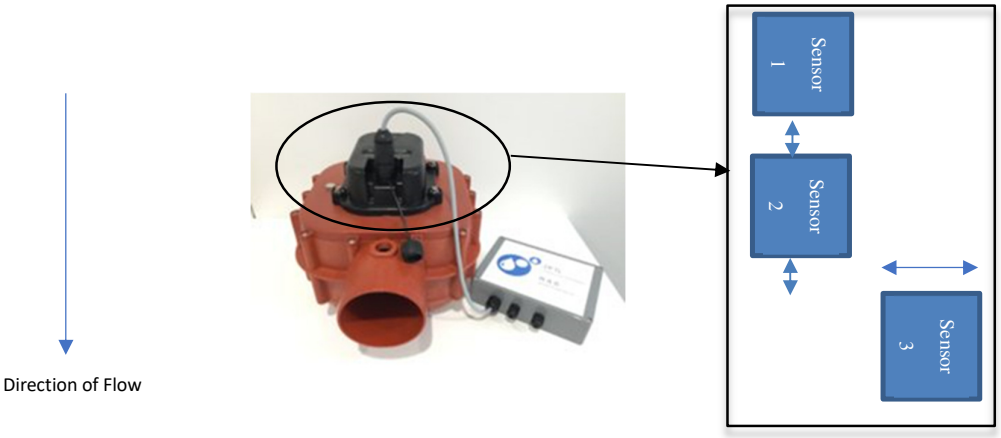


Figure 3. The microwave instrumentation consists of a sensor, remote access service (RAS) and a laptop with data control software.

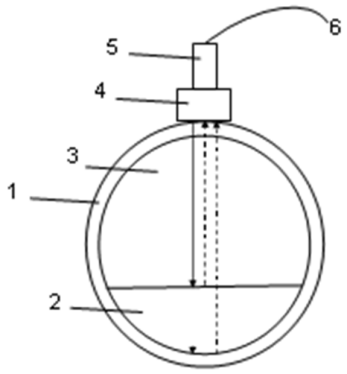


Figure 4. MWM principle of operation. The numbers correspond to 1—pipe, 2—variable water level, 3—air space, 4—waveguide interface to the pipe, 5—microwave sensor, and 6—connector cable to electronic instrumentation. The solid vertical arrow is the emitted signal while the dotted vertical arrows are the reflected signals.

A series of tests of several different types of microwave water-level sensors were carried out by [12] the National Oceanic and Atmospheric Administration (NOAA) Centre

for Operational Oceanographic Products (CO-OPS) in order to gain an understanding of sensor functions and performance capabilities. The experiments were conducted at the National Surface Warfare Centre (NSWC) Mask Facility in Carderock (Maryland, USA), and resulted in the collection of a unique and valuable data set for assessing the impact of surface waves on microwave meter readings. For most of the test runs, the sensors performed well, measuring water levels within 1 cm accuracy in the presence of ocean waves [12]. In Ref. [13], a low-cost microwave device (microstrip line technique) was developed that operated at high frequencies for detecting humidity levels in a gas line. The sensor showed a high sensitivity to humidity (5 kHz per %Relative Humidity) and good reversibility, i.e., returning to initial conditions without hysteretic behavior.

The objective of this paper is to determine whether a newly developed microwave sensor can be used to reliably estimate, in real time, discharges in pipes running partially full. To achieve this, validation data were obtained by conducting a series of experiments across a range of pipe flow depths (0.05–0.9) D, D = pipe diameter, with two different slopes and pipe diameters. The microwave sensor data were then used in combination with the Chezy, Manning and Colebrook–White equations to predict the discharge. The accuracy of the predictions was then evaluated against separate, direct measurements of discharges.

2. Materials and Methods

2.1. Experimental Details

The test rig in Figure 1 was constructed just outside the Hydraulics Laboratories at Loughborough University. The 21 m-long experimental "sewer" was constructed from 101.6 and 152.4 mm-diameter PVC pipes, supported on scaffolding tubes and providing a gentle slope of 1°, the industry-recommended minimum for wastewater pipes [14]. A second set of experiments was also performed on a slightly steeper slope of 2°. A 3 m-long, 101.6 mm-diameter translucent pipe was used for observations. This clear section was positioned immediately before the microwave meeting for visualizing flow conditions. While the aim is to develop a microwave meter for measuring wastewater flows under gravity drainage, the current experiments used clear water in order to first test the reliability of the meter without the additional complexity of dealing with either dissolved or solid contaminants, or the effects of humidity, temperature, and viscosity. The impact of these effects and the variability of sediments and debris on sensor performance will be considered in a future paper. Clear water was pumped from the laboratory sump to a 10 m-high tower tank, from where it flowed via gravity through an electromagnetic flowmeter (reference meter) and then into the experimental test rig. Flow was controlled by a manual gate valve, with an accuracy of 2–3%. The reference meter (Siemens Danfoss xyz, RS Hydro UK) was positioned before the feeder tank and was calibrated against a BSI-certified weigh tank (Avery ABC, Avery UK) with an accuracy of 3.17 g, corresponding to a water volume of 0.003 m^3. The typical correlation R^2 was between 0.9603 and 0.9916, and it varied with flow rate and depth. At the bottom of the feeder tank, the flow was taken through honeycomb baffles in order to readjust the flow to near normal conditions as it entered the 7 m pipe test section. The microwave meter was placed 6 m downstream of the feeder tank.

The experiments were designed to investigate the effects of flow rate, slope, and pipe diameter on the ability of the microwave sensor to reliably measure discharge. Pictures of the pipe system are shown in Figure 1, with a corresponding schematic given in Figure 2. On the bottom right-hand side of Figure 1, the electromagnetic reference meter used for comparison is clearly visible. The microwave meter (also shown enlarged) is visible on the left-hand side of Figure 1.

The microwave meter is shown in Figure 3, along with a schematic in Figure 4 showing the layout of the sensor operation. The meter consists of three microwave sensors placed

equidistant in the head of the meter and parallel to the direction of the pipe flow. Each of these sensors is based on a dielectric resonator, a stabilized microwave FET (field effect transistor), and an oscillator in the X-band. The microwave meter operates according to the Doppler radar principle by transmitting a continuous signal of low-energy microwave radiation at the target area and then analyzing the phase of the reflected signal, which provided a high-resolution 0.1 mm measurement capability for the water height. The detector operates at a frequency of 10 GHz. Calibration of the meter was then obtained by combining the sensor data with a range of separate laboratory experiments on a test rig with known discharges and slopes.

The flow conditions during testing are summarized in Table 1 below and represent a range of flow rates (based on real flows that a gravity drainage system might experience) for the pipe. While the Reynolds number range was not large, it is similar to that used in other partially filled pipe flow studies. For example, Ref. [2] considered a range of (1.9–8.6) x 10^5, while direct numerical simulations by Ref. [15] and large-eddy simulations by Ref. [16] were for bulk Reynolds numbers in the ranges of 3240–15,452 and 17,000–19,000, respectively.

Table 1. Summary of main hydraulic parameters for the experiments.

Parameters	Range
Discharge, Q (L/s)	0.6–22.6
Reynolds number, R_e	(0.27–3.25) $\times$ 10^5
Froude number, F_r	1.5–3.6

2.2. Theory

To optimize the quality of the flow measurements, a measurement section was selected where normal flow conditions were expected to occur. Since the depth (h) at the inlet is known, the position where normal depth occurs can be found by integrating the gradually varying flow equation in the form:

$$\frac{d\theta}{dx} = \frac{\left(S_0 - S_f\right)}{\frac{dh}{d\theta}\left(1 - F_r^2\right)}, \quad F_r^2 = \frac{Q^2 T}{gA^3}, \tag{1}$$

where x is the distance down the pipe; θ ($0 \leq \theta \leq \pi$) is the angle to where the water surface intersects the edge of the pipe with a dry, half full, and full pipe, given by $\theta = 0$, $\theta = \pi/2$, and $\theta = \pi$ respectively; T (m) is the top width of the free surface; A (m^2) is the cross-sectional area of the flow; and F_r is the Froude number. The angle θ was chosen as the dependent variable to remove the need for iteration in determining terms on the right-hand side of Equation (1), which are found from:

$$A = r^2(\theta - \sin\theta\cos\theta), \tag{2}$$

$$T = D\sin\theta, \quad h = r(1 - \cos\theta), \tag{3}$$

$$P = 2r\theta, \quad R = \frac{r}{4}\left(2 - \frac{\sin 2\theta}{\theta}\right), \tag{4}$$

where r is the pipe radius (m), D is the pipe diameter (m), h is the flow depth (m), P is the wetted perimeter (m), and R is the hydraulic radius (m).

Taking Manning's metric equation for S_f:

$$S_f = \frac{n^2 Q^2}{A^2 R^{4/3}}, \tag{5}$$

with a typical value of the roughness coefficient of n = 0.009 for a PVC pipe, for the range of discharges from Table 1, positioning the meter 6 m downstream from the baffles would ensure that essentially normal flow conditions in the pipe would be realized.

Given that the data were collected under normal flow conditions, in addition to the application of Manning's equation, we were also interested to see whether the Chezy equation can be used to analyze the data. The Chezy equation is applicable to both uniform equilibrium and gradually varied turbulent flows [17], and is given by:

$$Q = CA(RS_0)^{1/2}, \tag{6}$$

where C is the Chezy coefficient:

$$C = \sqrt{\frac{8g}{f}}, \tag{7}$$

where f is the friction factor (-) and g is gravity (m/s^2). This is suitable for partially filled pipes provided the surface is moderately hydraulically smooth and the pipe diameter is small and less than 0.25 m [18].

In general, f is not constant but rather is a function of the flow Reynolds number (R_e) and the relative roughness (k_s/D_H) of the channel/conduit, and is given through the Colebrook–White formula as:

$$\frac{1}{\sqrt{f}} = -2\log_{10}\left(\frac{k_s}{3.71 D_H} + \frac{2.51}{R_e\sqrt{f}}\right), \tag{8}$$

where the Reynolds number is given by:

$$R_e = \frac{V D_H}{\nu}, \quad D_H = 4R, \tag{9}$$

and where $V = Q/A$ is the bulk flow velocity (m/s), D_H is the hydraulic diameter (m), ν is the kinematic viscosity (m^2/s), and k_s is the surface roughness measure (m). Combining Equations (6), (7), and (9) yields:

$$R_e\sqrt{f} = \frac{D_H}{\nu}\sqrt{8gRS_0}, \tag{10}$$

which, with Equation (8), allows for the friction factor under normal flow conditions to be obtained explicitly as:

$$\frac{1}{\sqrt{f}} = -2\log_{10}\left(\frac{k_s}{3.71 D_H} + \frac{2.51\nu}{D_H\sqrt{8gRS_0}}\right). \tag{11}$$

While the Colebrook–White formula was developed for full pipe flow, it has been commonly applied to open channel flow. In a study on laminar and turbulent flow in partially filled pipes, Ref. [1] suggested that to facilitate a direct comparison with full pipe flow, the Reynolds number should be based on an equivalent diameter D_{EQ} rather than D_H. D_{EQ} is the equivalent hydraulic diameter for a full pipe with the same flow cross-sectional area of the semi-filled pipe and is given by:

$$D_{EQ} = 2\sqrt{\frac{A}{\pi}} = \frac{2r}{\sqrt{\pi}}(\theta - \sin\theta\cos\theta)^{1/2}. \tag{12}$$

By replacing D_H with D_{EQ} in Equations (9)–(11), we obtain a modified Colebrook–White formula that can also be tested against the experimental data. We adopt the terminology of CW_H for Equations (9) and (11) and CW_{EQ} when Equation (12) is used in place of D_H. Thus, in total we have four different discharge equations: Manning, Chezy C with a constant friction factor, CW_H, and CW_{EQ}, which can be combined with the microwave meter readings and be evaluated against the measured data.

2.3. Data Collection

All experiments were performed under the same environmental conditions using clear water. Data from the microwave meter were collected using a remote access service (RAS) and transferred to servers using Bluetooth technology. Data from the reference flowmeter were collected using a conventional data logger. All data were processed with MATLAB R2023b software (MathWorks, Natick, MA, USA). The volumetric flow through the pipe was varied in a cyclic pattern through time, as shown below in Figure 5, with each data point measured after steady flow conditions were visually observed. This was carried out to test for reproducibility in the microwave meter by approximately replicating flow rates.

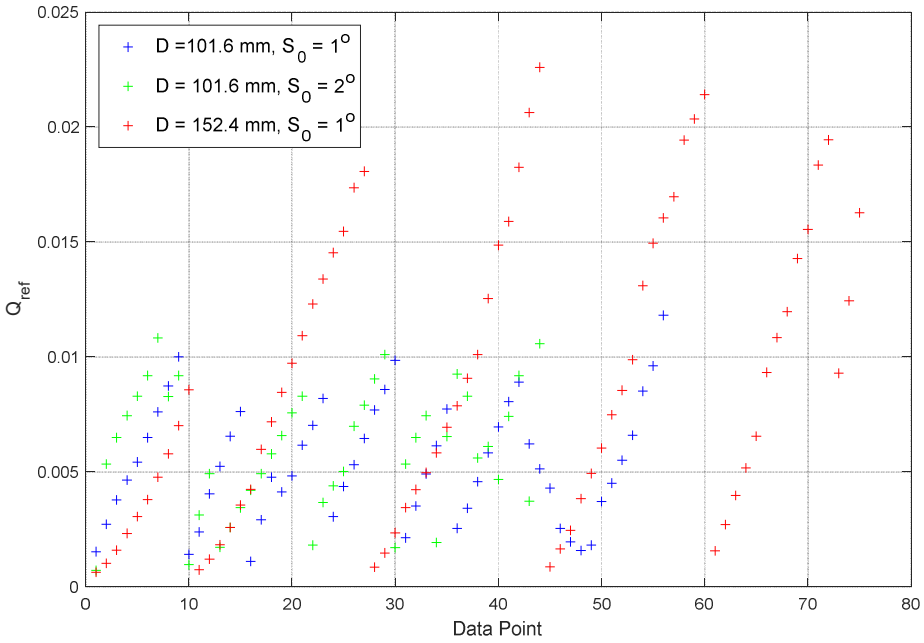


Figure 5. Temporal pattern of varying discharge flow rates for the three different pipe diameter and slope experiment combinations. Q_{ref} is the discharge measured by the reference meter.

Photogrammetry was also used to determine the shape of the water surface in the pipe, whereby surface waves of approximately 2.5 mm were found. The effect of surface waves of up to 10 mm on measurement reliability were investigated, and it was found that these could be resolved up to an accuracy of 0.1 mm. To minimize the impact of surface waves on measuring flow depth, a large amount of data were collected (20 readings/sec) over approximately 3 min for a set flowrate. The average value of these readings was then used to determine the flow depth.

3. Results

As noted previously, the microwave meter is calibrated to provide estimates of the flow depth h. With h being known, both the flow area A and the hydraulic radius R can be found through Equations (2)–(4). Overall, 175 separate discharge experiments were carried out. A least-squares analysis was used to determine the parameter n for the Manning equation

(Equation (5) with $S_f = S_0$), the Chezy equation with a constant C, or the Chezy equation with k_s, using either CW_H or CW_{EQ} for the best least -squares estimate of the measured discharge. The results of this analysis across all three pipe setups for the four different discharge equations along with the resulting parameter values are shown in Figure 6 using the dimensionless discharge Q_d, given by:

$$Q_d = \frac{Q}{D^2(gDS_o)^{1/2}}. \tag{13}$$

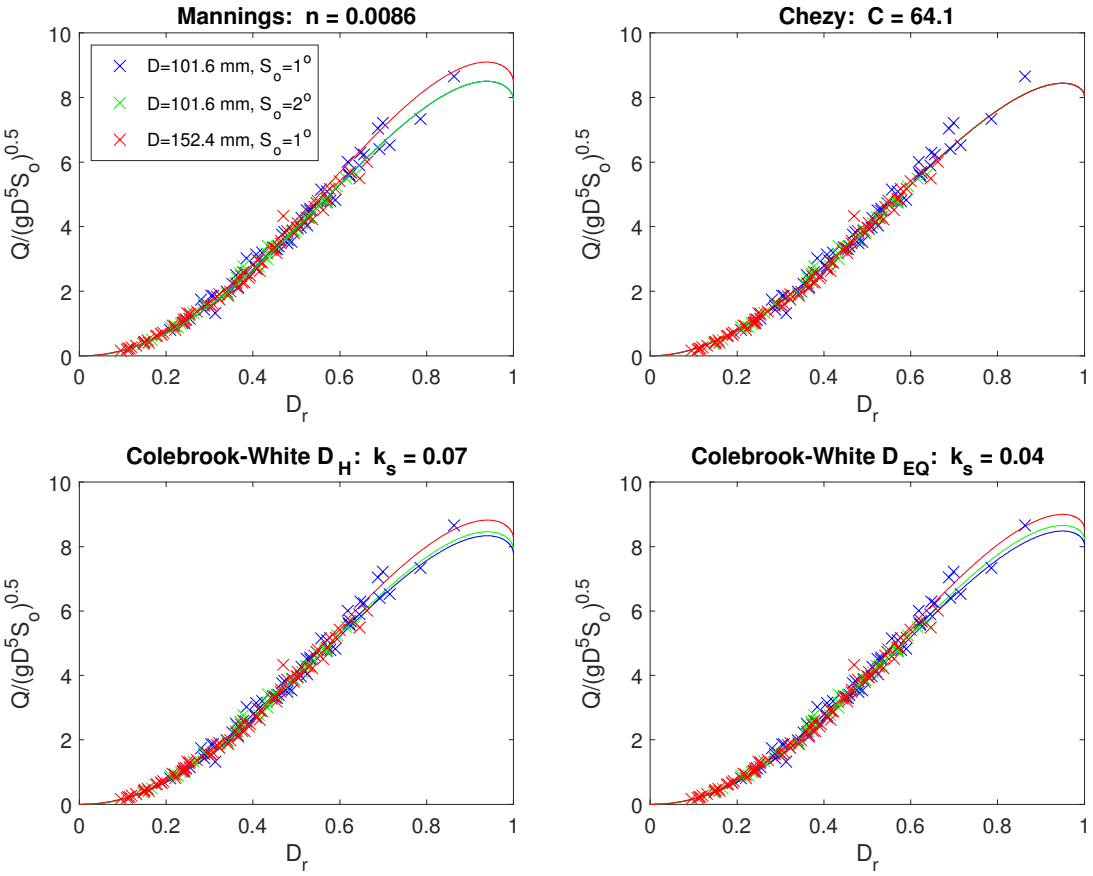


Figure 6. Comparison of measured reference data (symbols) against predicted discharge (solid lines) for three different experimental conditions, as indicated in the legend, as a function of relative flow depth $D_r = h/D$. The corresponding parameters, n, C, and k_s, were determined via least squares.

We note that for the Chezy law, this scaling will result in Q_d being independent of both the pipe diameter and slope, and only depends on θ and the constant value for f. However, there will still remain a slight D dependence for the Manning equation ($D^{1/6}$) and for the Colebrook–White formulations through both D_H and D_{EQ} via Equation (11), which is why multiple curves appear for these particular cases in Figure 6.

An alternative approach to processing the data is to calculate the value of the parameter that matches exactly onto the data point and plot the corresponding frequency distribution. For example, for each measured Q from a given pipe diameter and slope experiment, the Manning equation can be rearranged to find the corresponding n, and then the distribution of n values for that experiment can be produced. This can be repeated for each discharge law with the various histogram distributions presented in Figure 7. Using both versions of the Colebrook–White formula, Figure 8 presents the results of the friction factor as a function of the Reynolds number $f(R_e)$.

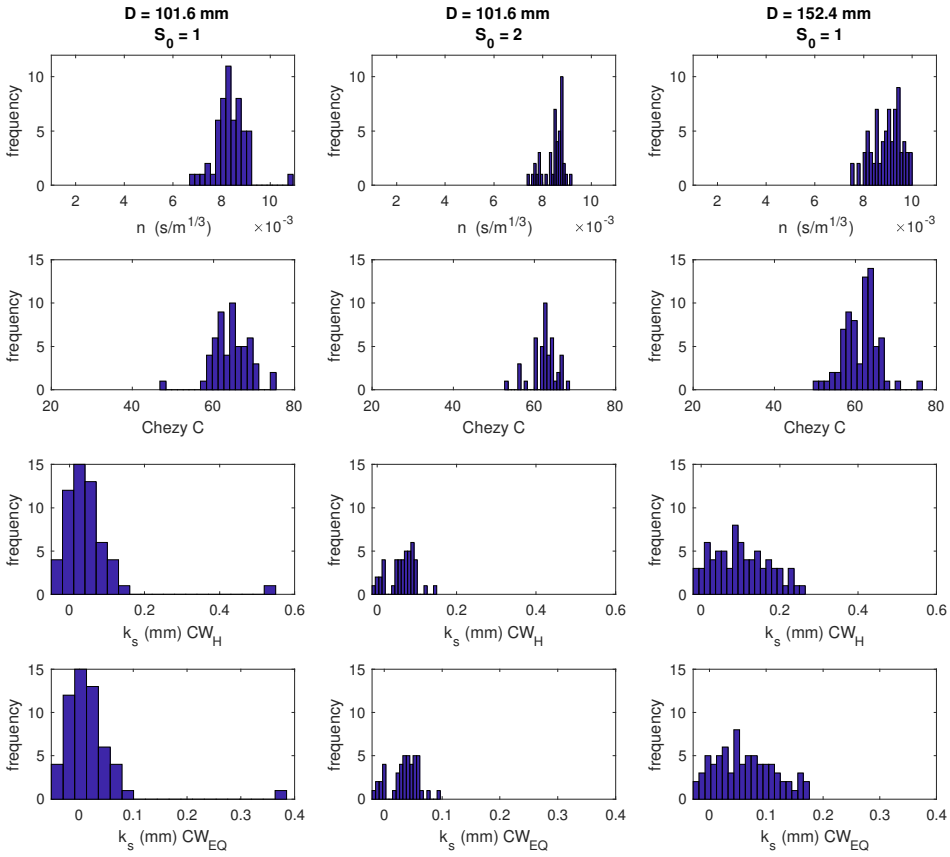


Figure 7. Frequency distributions for n, Chezy C, and k_s for the two versions of the Colebrook–White formula.

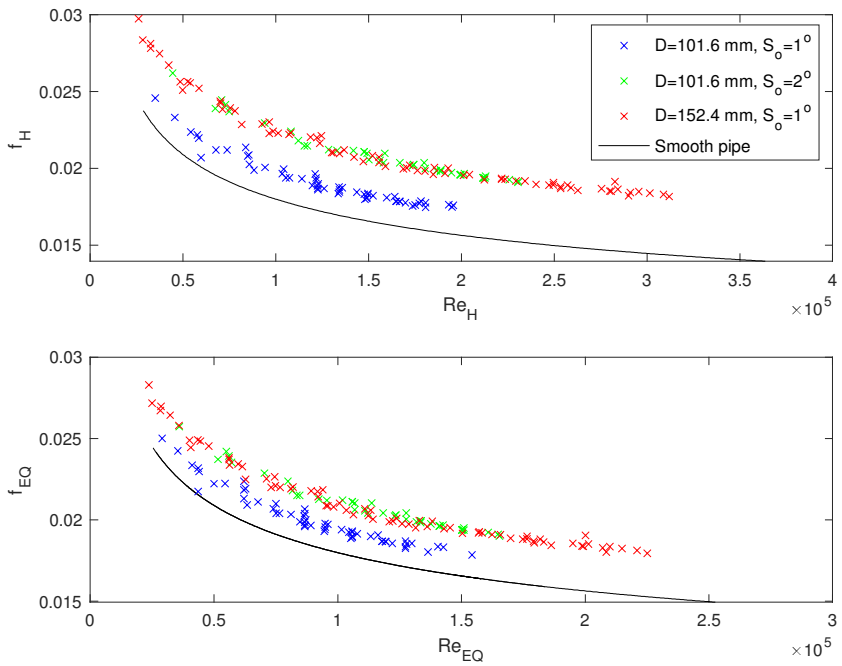


Figure 8. Plots of $f(R_e)$, where subscripts H and EQ refer to using either D_H or D_{EQ} in the Colebrook–White formula, respectively. The solid black line corresponds to the smooth pipe case of $k_s = 0$.

Figure 9 highlights the relationship between the Froude number with relative depth $F_r(D_r)$, the dependence between the Reynolds and Froude numbers $F_r(R_e)$ (data = crosses), and the theoretical curves resulting from both the Manning and the constant C Chezy

laws (solid lines). The theoretical curves are obtained by first rewriting both the Froude (Equation (1)) and the Reynolds (Equation (9)) equations as:

$$F_r = \frac{Q}{A}\sqrt{\frac{T}{gA}}, \quad R_e = \frac{Q}{A}\frac{4R}{\nu}, \tag{14}$$

and then noting that Q/A for the discharge laws can be written as:

$$\frac{Q}{A} = \alpha\sqrt{S_0}\, R^{\beta}, \tag{15}$$

where $\alpha = 1$, $\beta = 4/3$ for Manning, and $\alpha = C$, $\beta = 1$ for Chezy. For $0 < \theta < \pi/2$, Equations (2)–(4) allow $A(\theta)$, $T(\theta)$, and $R(\theta)$ to be calculated, along with $D_r = h(\theta)/D$, with $h(\theta)$ given by Equation (3), which permits the theoretical curves to be determined parametrically though θ.

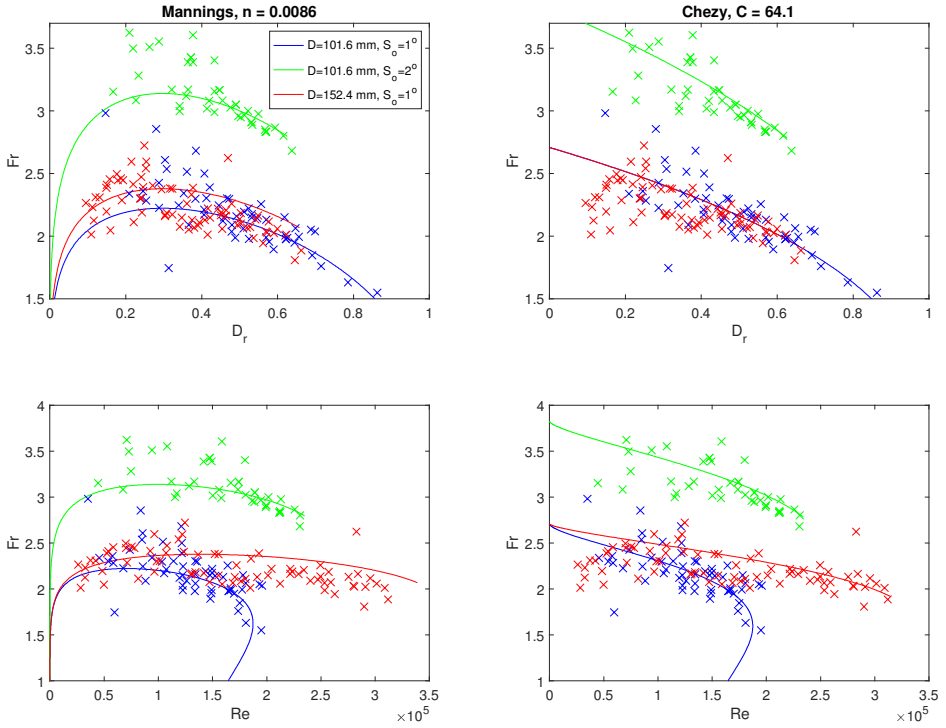


Figure 9. The top plot shows the Froude number as a function of the relative depth, with the bottom plot showing the Froude number's dependence on the Reynolds number. The solid lines are the theoretical curves using Manning's equation with n from Figure 6.

4. Discussion

From Figure 6, we see that there is a very good level of agreement between the predicted discharges based on all four discharge formulations and the measured discharge, with $R^2 > 0.98$ for all cases. The results in Figure 6 also cover a wide range of flow depths in the pipe, from low flow depths of D_r near 0.1 up to nearly 90% of the full pipe diameter. For the higher water levels, the predictions have an accuracy of approximately $\pm$ 5%, while for the lowest discharges, the accuracy varies within $\pm$ 15%. We also see that that there is quite a bit of scatter in the measured discharges. We believe that there are a couple of factors involved here. The 7 m pipe slope section that was used for the data collection was set using a total station and has a potential error of plus or minus 10%. The second reason is due to the experiments being conducted at high Froude numbers corresponding to supercritical flow with roll waves. These are very demanding conditions for any meter that obtains readings based on a reflected signal. In general, there is very little difference

between the magnitude of the differences across the various discharge relations. Due to the type of pump being used, it was not possible to reproduce experiments at the same discharge, but only at similar discharges, and therefore a direct measure of repeatability could not be obtained. However, we looked to overcome this issue by conducting the experiments with a series of increasing and decreasing pumping rates, or discharge cycles, as shown in Figure 5. This provided data at many similar pumping rates, and consequently, a good measure of the level of repeatability is demonstrated by the narrow spread of the experimental data in Figure 6.

The frequency distributions of n and C in Figure 7 are reasonably compact, and all closely centered approximately around n = 0.009 and C = 64. For C = 64, this results in a value for the friction factor of f = 0.019. The corresponding standard deviations going across the top two rows of Figure 7 are 0.00063, 0.00043, and 0.0006 for n and 4.6, 3.2, and 4.3 for C, respectively. However, when it comes to the distribution of k_s for the two bottom rows of Figure 7, they are quite broad, with a greater spread compared to n and C, and all of their corresponding standard deviations are of the same order of magnitude as their respective means. The distribution of k_s for CW_{EQ} is lower compared to CW_H because, for our data, D_{EQ} is nearly always considerably less than D_H. We note that for D = 101.6 mm and $S_0 = 1^\circ$, there is a single data point that sits well away from the main distribution, and we see this as an isolated outlier.

While typical published values for PVC pipes give values for k_s as approximately 0.0015 mm, our values are at least an order of magnitude greater and would normally reflect pipes made of steel. A range of $0.01 < k_s < 0.02$ mm for PVC pipes was given by Ref. [17], and while this is still smaller than what we obtained, we are at least in the same order of magnitude. However, while our k_s is high, Figure 7 shows that the Moody-style plots for both CW_{DH} and CW_{EQ} agree with the Moody diagram for the range of our experimental Reynolds numbers. A possible explanation, therefore, for the high k_s is that because of the supercritical flow and presence of roll waves, not all energy losses are just from the boundary shear stresses. Consequently, the effects of these additional losses are incorporated into k_s through the least-squares process and thus make k_s more of a curve-fitting parameter. In addition, Ref. [19] on p. 427 noted that tabulated k_s values correspond to new, clean pipes and that "after considerable use, most pipes (because of buildup of corrosion or scale" may have a relative roughness that is considerably larger (perhaps by an order of magnitude)." Given that our experimental pipe rig has been outdoors for several years in all weather conditions with numerous experimental runs, our k_s values tend to align with the comments of Ref. [19]. On p. 22 of Ref. [20] it was noted that the resistance to a uniform, steady flow is only a function of the Reynolds number and k_s, provided that the Froude number is not high, and its effect is negligible.

In experiments on partially full pipes, Ref. [4] looked at the effect of F_r on boundary shear stress distributions and found only a minimal effect, though their similar experiments were also subcritical. In Figure 9, the highest Froude numbers for Manning's equation occurred for a D_r of around 0.3, with F_r decreasing for both $D_r < 0.3$ and $D_r > 0.3$. For the Chezy law, F_r is at maximum at zero depth and decreases as D_r increases, which is quite different than the behavior exhibited by Manning's equation. By expanding both formulas for $D_r \to 0$, or equivalently $\theta \to 0$, then it is straightforward to show that for the Chezy law, F_r approaches the constant $C(S_0/g)^{0.5}$, while for the Manning law, it approaches zero as proportional to $\theta^{1/6}$. However, for the range of data shown in Figure 9, either the Manning or the Chezy laws are equally acceptable in representing the data. It is also worth noting that in the limit of θ near zero, neither the Chezy nor the Manning law apply, as we are now in the realm of thin film flow, where surface tension effects are far more important. Figure 4 of Ref. [1] has F_r increasing with R_e at subcritical flows but remaining constant for

weakly supercritical flow. This essentially agrees with the theoretical prediction from the Manning equation for subcritical flow and with our data for supercritical flows (Figure 9). However, the solid theoretical lines based on the fitted Manning's n suggest that there is a slight decrease in F_r as R_e increases, especially for the smallest pipe diameter and slope.

In Figure 12 of Ref. [5], they show that C rapidly increased as the relative flow depth increased for $0 < D_r < 0.5$, followed by a very gradual increase to $D_r = 0.8$. Even though there is a degree of scatter in our data, it is difficult to see such a similar trend in our data. While the value for C of 64.1 is much higher than those in Ref. [5], who used an acrylic pipe, the Reynolds numbers from our experiments were an order of magnitude higher than theirs, which then led to a lower f, and therefore a higher C. A series of experiments in PVC pipes were also conducted by Ref. [21], with similar Reynolds numbers at both sub- and supercritical flow. Unfortunately, the $F_r > 1$ experiments were conducted with a flat horizontal section inserted at the bottom of the pipe and are therefore qualitatively different. However, for their subcritical experiments without a flat bottom section, they obtained a similar distribution to Figure 8 for the friction factors as a function of D_r primarily centered around $f = 0.02$ (see Figure 19 of [21]). As seen in Figure 8, $f = 0.02$ sits approximately in the mid-range of each of the three pipe cases, and given the relatively small range of Reynolds numbers, it is therefore not surprising that a constant Chezy C value of around 64 provides a good match to the data (Figure 6).

According to Ref. [22], "The results of the 25 field measurements taken from four different localities showed that the value of Manning's n should be taken equal to 0.009 for a PVC pipe." The findings of Ref. [22] very much agree with our curve-fitted values of Manning's n in Figure 6. Indeed, it strongly suggests that for PVC pipes, the microwave readings can simply be combined with tabulated n values to estimate the pipe discharge. There have been several previous studies by Refs. [5,23,24] where it has been found that the Manning's n will vary depending on the relative depth of fluid in the pipe. Data obtained from Ref. [5] have shown n to be a decreasing function for flow depths that are less than the pipe radius, and almost constant for flow depths greater than the pipe radius. Data provided in Refs. [23,25] showed n to be a concave down function of the relative depth. However, there is also additional support for a constant n by Ref. [2] obtained from experiments on partial flow in a circular corrugated pipe of $D = 0.622$ m. They obtained a value of $n = 0.023$ for three different slopes of 0.55, 1.14, and 2.55% and relative flow depths of $D_r < 0.55$. This behavior has also been confirmed through field tests in sanitary sewers by Ref. [22].

For Manning's n, Figure 12 of Ref. [5] showed a decrease in D_r for $0 < D_r < 0.5$ and then remained relatively constant. Similar to our findings for C, our results for n do not show the same behavior as those of Ref. [5] and suggest that n could be taken as a constant. However, we also note that their experiments were all run at subcritical flows with $F_r < 0.55$, as opposed to our range of $1.5 < F_r < 3.6$. Interestingly, Ref. [26] comments that an advantage of Manning's n is "its near invariance over its values over a wide range of flow depth or hydraulic radius for fully developed turbulent, steady, uniform flow in straight circular pipes or wide, straight, prismatic open channels of impervious fixed boundary", which essentially agrees with our findings of using a constant n (Figure 6).

5. Conclusions

A range of experiments were carried out to test the ability of a microwave water meter to measure pipe discharges under varying flow depths. Two different pipe diameters and pipe slopes were considered. By plotting the dimensionless discharge against the relative flow depth for all 175 experimental runs, very good agreement between the data and the meter predictions were obtained. It was found that either the Chezy law with a constant

friction factor or Manning's law could be used in conjunction with the microwave sensor readings to provide reliable discharge predictions compared to the measured discharge. Of these six fits to the data, all of the R^2 values obtained from the plots of predicted versus measured discharge were greater than 98%.

It was found that the Colebrook–White formula in conjunction with either the hydraulic diameter or the equivalent diameter for full pipe flow could also be used to match the data. However, it was found that the resulting roughness coefficient was significantly larger than values typically used for a PVC pipe. In contrast, for Manning's law, recommended tabulated values for n were a good match to those obtained for our data. This suggests that for smooth PVC pipes, anyway, Manning's equation could also be used in a totally predictive capacity.

We have demonstrated the potential for our microwave sensor to provide a reliable prediction for the discharge under fully turbulent flow in a PVC pipe; however further experiments are required to test discharge predictions from the sensor under transitional and fully developed rough, turbulent flows in different types of pipes. From such experiments, we should be able to identify the reliable discharge-operating regime of the microwave sensor and whether Manning's law with tabulated values for n can still provide the same accuracy of discharge prediction when combined with the microwave sensor readings. Lastly, the meter was only tested with clear water flows, and much further research is also required to evaluate the meter using true wastewater flows under real-world conditions containing debris loads at various concentrations and temperatures, where the dialectic permittivity is likely to be quite different.

Author Contributions: Conceptualization, methodology, validation, and formal analysis: all authors; investigation, V.K., D.W. and M.C.; writing—original draft preparation and editing, V.K., G.S. and A.E.-H.; software, V.K. and G.S.; supervision, G.S., A.E.-H., D.W. and M.C. All authors have read and agreed to the published version of the manuscript.

Funding: We would like to thank the UK Engineering and Physical Sciences Research Council (EPSRC) and the Centre for Innovative and Collaborative Construction Engineering (CICE) at Loughborough University for the provision of a grant (number EPG037272) to undertake this research project in collaboration with Dynamic Flow Technologies Ltd.

Data Availability Statement: The raw data supporting the conclusions of this article will be made available by the authors on request.

Conflicts of Interest: Authors Duncan Wallace and Martin Croft were employed by Dynamic Flow Technologies Ltd. The remaining authors declare that the research was conducted in the absence of any commercial or financial relationships that could be construed as a potential conflict of interest.

References

1. Ng, H.C.H.; Cregan, H.L.F.; Dodds, J.M.; Poole, R.J.; Dennis, D.J.C. Partially filled pipes: Experiments in laminar and turbulent flow. *J. Fluid. Mech.* **2018**, *848*, 467–507. [CrossRef]
2. Ead, S.A.; Rajaratnam, N.; Katopodis, C.; Ade, F. Turbulent Open-Channel Flow in Circular Corrugated Culverts. *J. Hydraul. Eng.* **2000**, *126*, 750–757. [CrossRef]
3. Cunliffe, C.J.; Dodds, M.; Dennis, D.J.C. Flow correlations and transport behaviour of turbulent slurries in partially filled pipes. *Chem. Eng. Sci.* **2021**, *235*, 116465. [CrossRef]
4. Knight, D.W.; Sterling, M. Boundary Shear in Circular Pipes Running Partially Full. *J. Hydraul. Eng.* **2000**, *126*, 263–275. [CrossRef]
5. Yoon, J.-I.; Sung, J.; Ho Lee, M. Velocity profiles and friction coefficients in circular open channels. *J. Hydraul. Res.* **2012**, *50*, 304–311. [CrossRef]
6. Wada, S.; Furuichi, N.; Shimada, T. Development of ultrasonic pulse-train Doppler method for velocity profile and flowrate measurement. *Meas. Sci. Technol.* **2016**, *27*, 115302. [CrossRef]
7. Swaffield, J.A.; Bridge, S. Applicability of the Colebrook-White Formula to Represent Frictional Losses in Partially Filled Unsteady Pipeflow. *J. Res. Natl. Bur. Stand.* **1983**, *88*, 389. [CrossRef]

8. Tezuka, K.; Mori, M.; Suzuki, T.; Kanamine, T. Ultrasonic pulse-Doppler flow meter application for hydraulic power plants. *Flow Meas. Instrum.* **2008**, *19*, 155–162. [CrossRef]
9. Tareq Bin, M. Development of Acoustic Sensor and Signal Processing Technique. Available online: https://bradscholars.brad.ac.uk/handle/10454/4908 (accessed on 25 July 2024).
10. Larrarte, F.; Bardiaux, J.B.; Battaglia, P.; Joannis, C. Acoustic Doppler flow-meters: A proposal to characterize their technical parameters. *Flow Meas. Instrum.* **2008**, *19*, 261–267. [CrossRef]
11. Korostynska, O.; Mason, A.; Al-Shamma'A, A. Microwave sensors for the non-invasive monitoring of industrial and medical applications. *Sens. Rev.* **2014**, *34*, 182–191. [CrossRef]
12. Boon, J.D.; Brubaker, J.M. Acoustic-microwave water level sensor comparisons in an estuarine environment. In Proceedings of the OCEANS 2008, Quebec City, QC, Canada, 15–18 September 2008. [CrossRef]
13. Bernou, C.; Rebière, D.; Pistré, J. Microwave sensors: A new sensing principle. Application to humidity detection. *Sens. Actuators B Chem.* **2000**, *68*, 88–93. [CrossRef]
14. Water, U.K. Sewerage Sector Guidance-Approved Documents | Water UK. Available online: https://www.water.org.uk/sewerage-sector-guidance-approved-documents (accessed on 25 July 2024).
15. Brosda, J.; Manhart, M. Numerical investigation of semifilled-pipe flow. *J. Fluid. Mech.* **2022**, *932*, A25. [CrossRef]
16. Liu, Y.; Stoesser, T.; Fang, H. Effect of secondary currents on the flow and turbulence in partially filled pipes. *J. Fluid. Mech.* **2022**, *938*, A16. [CrossRef]
17. Chanson, H. *The Hydraulics of Open Channel Flow: An Introduction: Basic Principles, Sediment Motion, Hydraulic Modelling, Design of Hydraulic Structures*, 2nd ed.; Butterworth Heinemann: Oxford, UK, 2004; pp. 1–585. [CrossRef]
18. Henderson, F.M. *Open Channel Flow*; Macmillian: New York, NY, USA, 1966.
19. Munson, B.R.; Okiishi, T.H.; Huebsch, W.W.; Rothmayer, A.P. *Fluid Mechanics, SI Version*, 7th ed.; Wiley: Singapore, 2013.
20. Yen, B.C. Open Channel Flow Resistance. *J. Hydraul. Eng.* **2002**, *128*, 20–39. [CrossRef]
21. Sterling, M.; Knight, D.W. Resistance and boundary shear in circular conduits with flat beds running part full. *Proc. Inst. Civ. Eng. Water Marit. Eng.* **2000**, *142*, 229–240. [CrossRef]
22. Bishop, R.R. Hydraulic Characteristics of PVC Pipe in Sanitary Sewers (A Hydraulic Characteristics of PVC Pipe in Sanitary Sewers (A Report of Field Measurements) Report of Field Measurements). 1978. Available online: https://digitalcommons.usu.edu/water_rep (accessed on 17 September 2021).
23. Camp, T. Design of sewers to facilitate flow. *Sew. Work. J.* **1946**, *18*, 3–16.
24. Enfinger, K.L.; Kimbrough, H.R. Scattergraph Principles and Practice a Comparison of Various Applications of the Manning Equation. In *Pipeline Engineering and Construction: What's on the Horizon?* American Society of Civil Engineers (ASCE): Reston, VA, USA, 2004; pp. 1–13. [CrossRef]
25. Akgiray, Ö. Simple Formulae for Velocity, Depth of Flow, and Slope Calculations in Partially Filled Circular Pipes. *Environ. Eng. Sci.* **2004**, *21*, 371–385. [CrossRef]
26. Yen, B.C. Dimensionally Homogeneous Manning's Formula. *J. Hydraul. Eng.* **1992**, *118*, 1326–1332. [CrossRef]

Disclaimer/Publisher's Note: The statements, opinions and data contained in all publications are solely those of the individual author(s) and contributor(s) and not of MDPI and/or the editor(s). MDPI and/or the editor(s) disclaim responsibility for any injury to people or property resulting from any ideas, methods, instructions or products referred to in the content.